*Journal of Earth Science, Vol. 25, No. 2, p. 371–378, April 2014* *ISSN 1674-487X*
*Printed in China*
DOI: 10.1007/s12583-014-0427-5

# Glacier Volume Calculation from Ice-Thickness Data for Mountain Glaciers—A Case Study of Glacier No. 4 of Sigong River over Mt. Bogda, Eastern Tianshan, Central Asia

**Puyu Wang*[1], Zhongqin Li[1, 2], Wenbin Wang[1], Huilin Li[1], Feiteng Wang[1]**
1. *State Key Laboratory of Cryospheric Sciences*, *Tianshan Glaciological Station*, *Cold and Arid Region Environment and Engineering Research Institute*, *Chinese Academy of Sciences*, *Lanzhou* 730000, *China*
2. *College of Geography and Environment Science*, *Northwest Normal University*, *Lanzhou* 730070, *China*

**ABSTRACT: The determination of total glacial volume is important for the observation of climatic change and its consequences such as global sea-level rise. The tongue area of Glacier No. 4 of Sigong River over Mt. Bogda, eastern Tianshan was surveyed by ground-penetrating radar (GPR) and real time kinematic (RTK)-global positioning system (GPS) during the summer campaign 2009. In order to calculate the glacier volume, both co-kriging algorithm and estimation based on the theory of perfectly plastic material were employed. Results indicated that the ice-thickness distribution of the investigated glacier ranges from 0 to 105.0 m, with the mean thickness of 27.6 m in 2009. The corresponding ice volume was ~0.076 km$^3$ (~0.068 km$^3$ water equivalent). The bedrock topography shows more undulating than the glacier surface. The difference of the calculated ice volume in this study and the estimated value from the empirical formula is large. Therefore, it is urgent to validate the applicability of the existing empirical formula.**

**KEY WORDS: ice volume, ice-thickness, GPR, Glacier No. 4 of Sigong River, Tianshan.**

## 1 INTRODUCTION

Under the global warming, glaciers are experiencing heavy ablation around the world. The monitoring and determination of ice-thickness distribution and total glacial volume are important for understanding the interactions between climate and the complex glacier system and essential for the development of projections of glacier extent, sea-level rise and mountain hydrology (Jevrejeva et al., 2008). When assessing future glacier retreat, the current ice volume is the most important initial condition. In addition, progress in modeling glacier dynamics, which has led from one-dimensional flowline models (Wallinga and Van de Wal, 1998; Greuell, 1992) to models describing the three-dimensional (3-D) field of glacier flow (Gudmundsson, 1999; Hubbard et al., 1998), still crucially relies on accurate results of ice-thickness distribution. However, measuring ice-thickness distribution of a glacier and deriving its total volume is a difficult task. Measurements of ice-thickness, such as radio-echo soundings or borehole require extensive fieldwork and are expensive, laborious and difficult because of topographical constraints. Therefore, only a small fraction of the world's glaciers and ice caps have been surveyed. In order to derive glacier volume, ice-thickness data are interpolated and the interpolation can involve additional information, such as topographic data and ice-dynamics considerations (e.g., Binder et al., 2009; Bauder et al., 2003; Funk et al., 1994). The continuous bedrock derived by the comparison of glacier surface and ice thickness can also be used to model glacier dynamics.

*Corresponding author: wangpuyu@lzb.ac.cn


Manuscript received September 2, 2013.
Manuscript accepted November11, 2013.

Ground penetrating radar (GPR) is a geophysical method, which is a rapid, high-resolution tool for non-invasive subsurface investigation. Since the 1970s, GPR surveys have been performed on permafrost and frozen soils, glacial ice, sea ice, sedimentary environments, rock, riverbeds, and lakebed deposits, snow accumulations for internal layering detection (Kouemou, 2010). In the 1980s, a radar-sounding system was designed at the Lanzhou Institute of Glaciology and Geocryology (LIGG), Chinese Academy of Sciences, and the ice-thickness of Ürümqi Glacier No. 1 was successfully surveyed (Zhang et al., 1985). With the rapid development of GPR, it has been used for the ice-thickness measurement of glaciers in the Chinese territory since the late 1990s (Wang and Pu, 2009; Sun et al., 2003). The combination of GIS, GPS and GPR allow data measurement, positioning and processing integrated, supplying reliable data for the determination of ice-thickness distribution and volume calculation. The empiri relations between glacier area and volume (e.g., Shi, 2005; Bahr et al., 1997) or glacier area and mean ice-thickness (e.g., Müller et al., 1976) can be used for the estimation of total ice volume for glaciers without direct ice thickness measurements.

Bogda region (43°44′N–43°53′N, 88°12′E–88°29′E) is the largest glaciated area in the eastern Tianshan, which contains 113 glaciers and a total area of 101.42 km$^2$, which assume highly localized distribution (~25 %) in this region (Shi, 2005).

Wang, P. Y., Li, Z. Q., Wang, W. B., et al., 2014. Glacier Volume Calculation from Ice-Thickness Data for Mountain Glaciers—A Case Study of Glacier No. 4 of Sigong River over Mt. Bogda, Eastern Tianshan, Central Asia. *Journal of Earth Science*, 25(2): 371–378, doi:10.1007/s12583-014-0427-5

Glaciers in this region preserve vital water resources, which are essential for oases and for the sustainable development of the ecological environment, industry, agriculture and tourism in this region. However, the climatic warming observed in China, especially since the 20th century, causes the mass loss for glaciers over Mt. Bogda during the recent decades (Li et al., 2010). Taking this into account, Tianshan Glaciological Station organized a scientific expedition in this region in July 2009. Glacier No. 4 of Sigong River (43°49′N, 88°21′E; Fig. 1; Glacier No. 4), a typical cirque-valley glacier, distributed on the northern slope of Mt. Bogda with an area of 3.33 km$^2$ and length of 3.2 km derived from the topographic maps in 1962 was surveyed by GPR and high-precision RTK (real-time kinematic)-GPS as a representative glacier. The main objectives of this work were to: (1) present the subglacial valley morphology from radar image and (2) investigate ice-thickness distribution, calculate ice volume, and construct the bedrock topography of Glacier No. 4. Although this study does not focus on a large number of glaciers, it presented an example for the calculation of glacier volume from ice-thickness data for mountain glaciers.

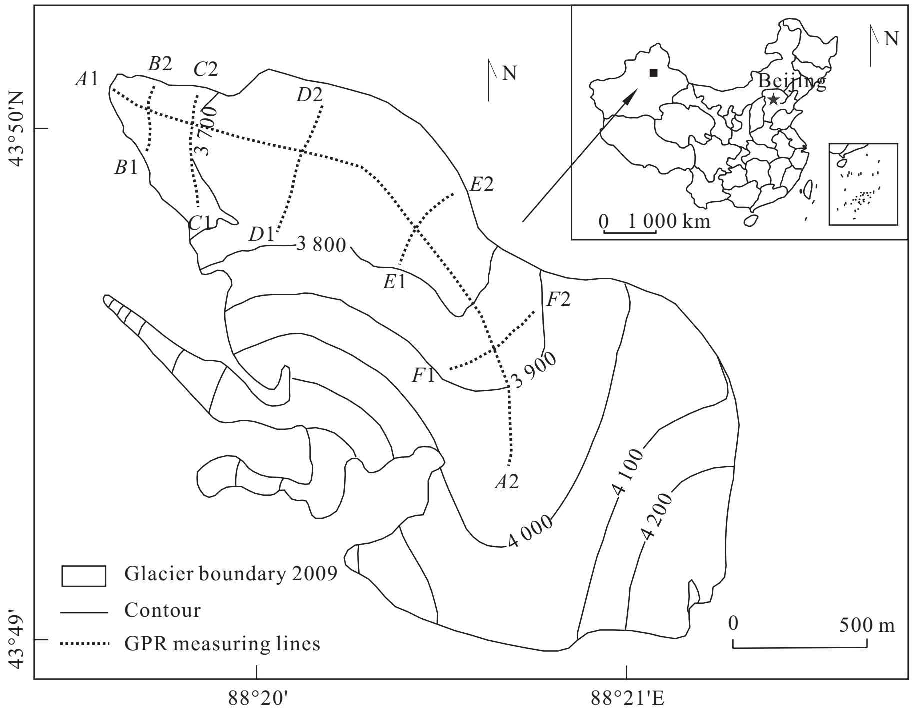


**Figure 1. Ice surface topography of Glacier No. 4 of Sigong River, over Mt. Bogda, Tianshan, central Asia in 2009 by in-situ measurement. Contour interval=100 m. The dotted lines indicate the measuring lines of GPR (five transversal profiles and one longitudinal profile along the flowline) in July 2009.**

## 2 DATA AND METHOD

### 2.1 Radar Survey and Data Processing

During the summer campaign 2009, GPR surveys were undertaken within the tongue area of Glacier No. 4. In very steep and/or crevassed areas, no measurements were carried out. The pulseEKKO 100 A enhancement radar system, made by Sensors and Software Inc., Mississauga, Canada, was employed, equipped with 100 MHz resistively loaded dipole antennae. The energy transmitted by this type of antennae is directional, with most power directed downwards in a plane perpendicular to the long axis of the antenna (Annan et al., 1975). Therefore, our surveys were undertaken with the antennae orientated perpendicular to the line of survey so that maximum power was transmitted in-line. In this way reflections from off-line were minimized, although it was still possible for high-conductivity surface features, such as survey poles, data loggers or streams, to produce reflections (Murray et al., 1997; Sensors and Soft Ware Inc, 1994).

For the tongue area, one longitudinal profile (*A*1*A*2) and five transversal profiles (*B*1*B*2; *C*1*C*2; *D*1*D*2; *E*1*E*2; *F*1*F*2) with a total of 641 points were generated from the measurement, as shown in Fig. 1. For this GPR survey a common-offset geometry with point measuring mode was used. The transmitting-receiving antennae were arranged parallel to each other at a distance of 4 m and transverse to the profile direction. The handheld approach is the most effective method for surveying. The irregular location of the GPR survey relates to the surface relief. The obtained GPR images (Figs. 2 and 3) clearly show the continuity of bedrock echoes.

The radar image of the longitudinal profile *A*1*A*2 are presented in Fig. 2. Figure 2a shows that the ice thickness varies along the flowline from the glacier terminus to approximate 3 900 m a.s.l., with the average thickness of 70.8 m. The radar image along the glacier flowline after elevation-calibration (Fig. 2b) gives visual information on the undulation of glacier surface and bedrock topography. Bedrock of the glacier fluctuates along the longitudinal profile with the rising altitude. Comparing with the glacier surface, the fluctuation of the bedrock is more dramatic, reflecting the strong glacial erosion processes on the bedrock. As a result, an obvious topographic depression is shaped with the maximum ice thickness of 105.0 m near to the altitude of 3 775 m a.s.l.. The difference of the undulation shapes of glacier surface and bedrock topography indicates that perturbations produced by Glacier No. 4 bedrock undulations are damped out before they reach the glacier surface. Hutter (1983) predicted the undulated wavelengths of the bedrock as three to five times as the glacier thickness must perturb the ice surface topography directly and the bedrock undulation will not impact the surface topography when its wavelength is too long or too short.

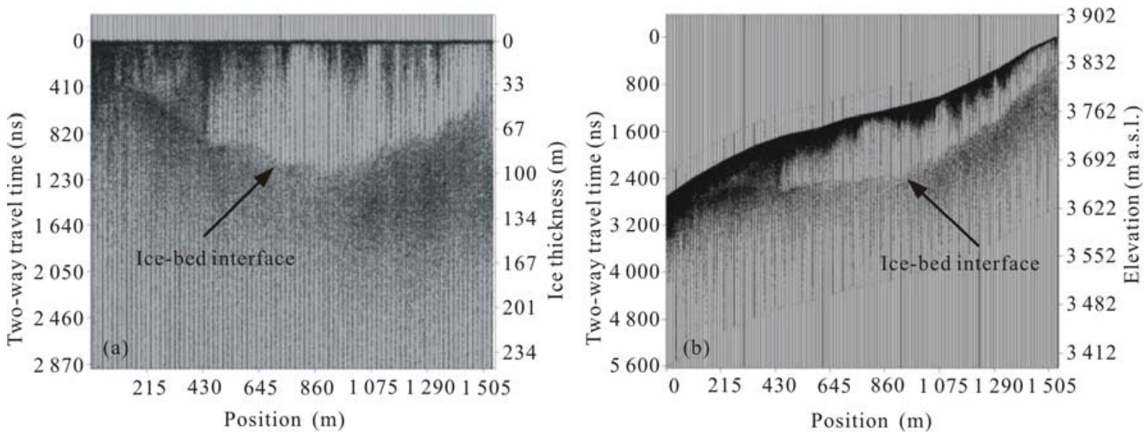


**Figure 2. Radar image of the longitudinal profile *A*1*A*2 (survey from the glacier terminus towards 3 900 m a.s.l.) of Glacier No. 4 of Sigong River. (a) Ice thickness distribution along the flowline; (b) glacier surface and bedrock topography, after elevation-calibration. The *x*-axis is the distance from the starting point of the survey.**

Radar image provide clear cross-sections of the subglacial valley. What need a specification is, the radar image of the transversal profile *B*1*B*2, located at the glacier terminus (Fig. 1), can not completely demonstrate the subglacial morphology due to the dramatic glacier melting and highly filled with water. Thus, in this study, it is not taken into consideration.

Figure 3 shows the radar images of the transversal profiles *C*1*C*2, *D*1*D*2, *E*1*E*2 and *F*1*F*2. In the profile *C*1*C*2 (Fig. 3a), the bedrock topography is generally flat and the ice thickness is thin, closely related to the steep slope. Generally, the steeper the glacier surface slope, the thinner the ice thickness (Paterson, 1994). *D*1*D*2 shows the non-symmetry subglacial valley with the southwest side steeper than the northeast side. *E*1*E*2 profile (Fig. 3c) shows the parabola-shaped subglacial valley in the tongue area of the glacier. The valley has steep sides and a narrow bottom at the area of maximum ice thickness indicating strong over-deepening glacier erosion. *F*1*F*2 (Fig. 3d) indicates the subglacial valley, near to the altitude of 3 875 m a.s.l., is flat and wide. The morphologies of subglacial valley cross-sections differ greatly in different parts of the glacier, which helps understanding the impacts of glacier valley cross-sections on the glacier motion.

The GPR data were processed in the software of EKKO_View Deluxe (professional version). On the 2-D radar image, the ice thickness ($h$) derived from vertical axis radar wave two-way travel time can be calculated by the expression

$$h = \frac{t_s}{2} \times v \tag{1}$$

where $t_s$ is the radar wave two-way travel time and $v$ is the velocity of radar signal in glacier. The propagation velocity was not determined at the measurement locations but was assumed to be 169 m·μs$^{-1}$ (Kovacs et al., 1995). This value is well within the range given in the literature (e.g., 167.7 m·μs$^{-1}$ (Glen and Paren, 1975); 168 m·μs$^{-1}$ (Narod and Clarke, 1994); 168.5 m·μs$^{-1}$ (Robin, 1975).

### 2.2 RTK-GPS Survey

Concurrent with GPR surveying, positional data were collected by RTK-GPS survey (Unistrong E650) during the summer campaign 2009, at a sampling spacing of 20–50 m. All GPS data, measured with respect to the Universal Transverse Mercator (UTM) World Geodetic System 1984 ellipsoidal elevation (WGS84), were re-projected and transformed to the 1954 Beijing Geodetic Coordinate system (BJ54) GEOID using Unistrong Landtop software (version 2.0.5.1). The method of measuring a surface point in the differential mode results in a survey error of ~0.10–0.30 m for geodetic-quality GPS receivers (Rivera et al., 2005). The error using seven-parameter model in the space transform model is less than 0.002 m (Wang et al., 2003). The datum level is the mean sea level of the Yellow Sea, namely, Qingdao Tidal Observatory. For the accumulation area, the surface topography is determined by interpolating data from neighboring areas located further up-glaciers, referring to Molina et al. (2007).

### 2.3 Accuracy of Ice-Thickness Measurements

The accuracy of ice-thickness measurements is determined by two factors: the accuracy of the measurement system and the properties of the ice and bedrock. For the first the resulting errors are small compared to the measured values, which is dependent on the accuracy of radar wave travel time and velocity. By analysis, the relative error of radar thickness ($h$) can be calculated by the equation (Sun et al., 2003)

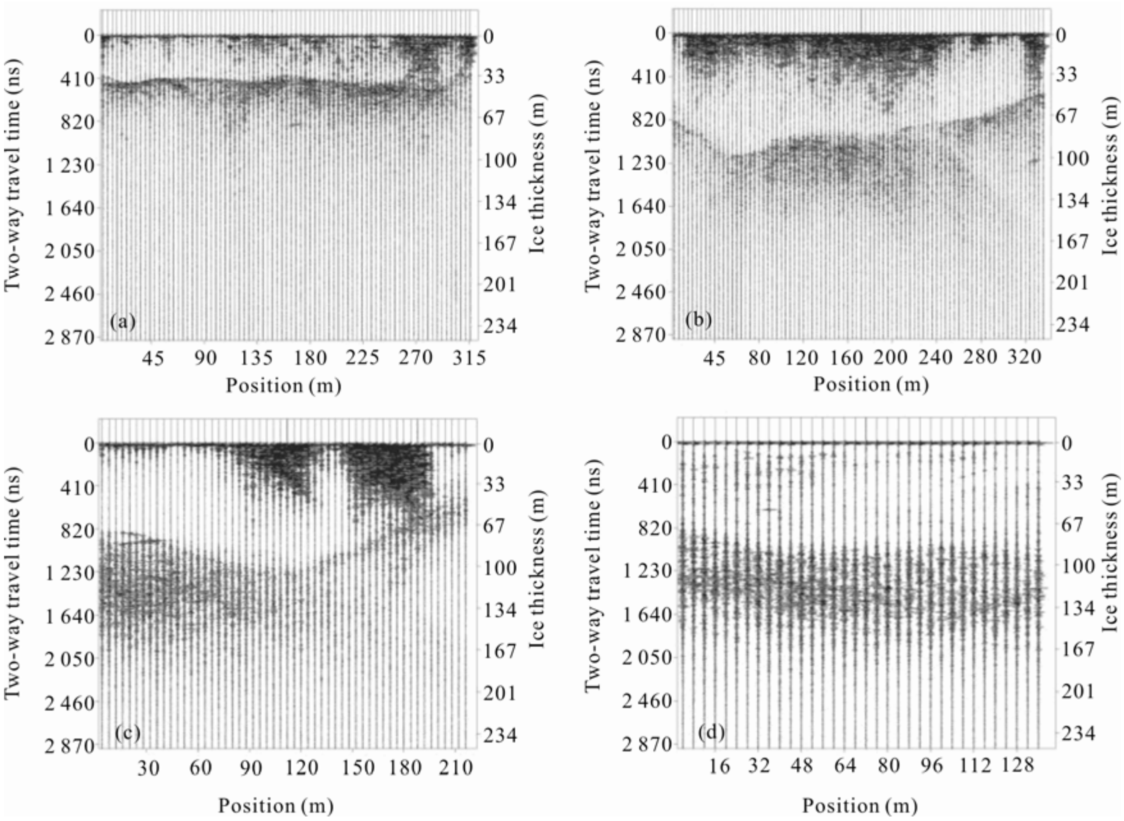


**Figure 3. Radar images of the transverse profiles (a) *C*1*C*2; (b) *D*1*D*2; (c) *E*1*E*2 and (d) *F*1*F*2 of Glacier No. 4 of Sigong River. The *x*-axis is the distance from the starting point of the survey.**

$$\frac{\Delta h}{h}=\frac{\Delta v}{2v}=1.2\% \tag{2}$$

The second source of error is more difficult to quantify and can have far larger effects on the ice thickness measurements. The internal structure of the glacier, including crevasses, internal boundaries and inhomogeneities, as well as topography and roughness of the bedrock, can cause large errors. In the case of multiple reflections, identification of the signal reflected from the bedrock can be difficult or even impossible. Bedrock undulations on the same order of magnitude as the ice thickness can lead to misinterpretation of the data. In addition, Haeberli et al. (1982) estimated the error introduced by neglecting firn layers at ~5%. Two topographic maps (1 : 50 000), derived from aerial photographs acquired in 1962 by the Chinese Military Geodetic Service and photos taken in the field observation were also used to determine larger-scale bedrock undulations, since ridges in the bedrock are often indicated by crevasse zones. Single points exhibiting unfavorable geometry can show far larger deviations, also affecting the total glacier volume. Therefore the data were carefully controlled and the spatial interpolation was based on the ice thickness after artificially eliminating.

## 3 DISTRIBUTION OF ICE-THICKNESS AND GLACIER VOLUME CALCULATION

Based on the constant basal shear stress assumption for steady-state glaciers and the approximation that ice is a perfectly plastic material, with a yield stress of 100 kPa (Paterson, 1994). For the highly crevassed area of Glacier No. 4, where radar profiling was not possible, ice thickness can be estimated using

$$H=\frac{\tau_0}{\rho g\sin\alpha} \tag{3}$$

where $H$ is the resulting ice thickness, $\tau_0$ the yield stress (100 kPa), $\alpha$ shape factor which accounts for drag on the valley side-walls and glacier bed (Nye, 1965), $\rho$ the ice density (900 $kg \cdot m^{-3}$), $g$ the acceleration due to gravity (9.81 $m \cdot s^{-2}$) and the corresponding optimum averaged surface slope field. In order to determine the ice-thickness distribution of Glacier No. 4, the co-kriging algorithm was used. The technique copes well with irregular data distribution and it can meet the interpolation challenge. Such an approach, commonly used in mineral exploration and geohydrology (McBratney and Webster, 1983), is amenable to glaciological applications. The method we adopt is applied to spatially irregular ice-thickness data generally collected along sections with the correlated glacier surface elevation data. The isolated radar ice-thickness can also be included. The basis for co-kriging interpolation is the cross-semivariogram, which characterizes the spatial variability of the studied characteristic. The ice thickness was taken to be zero at the margins, and a spherical semivariogram was assumed. The interpolation to calculate a raster of ice thickness, surface topography and bedrock topography, and other arithmetic were implemented in the commercial ArcGIS 9.3.

Based on the method mentioned above, the spatial distribution of ice-thickness for Glacier No. 4 is determined as shown in Fig. 4. The ice thickness of Glacier No. 4 ranges from 0 to 105.0 m, showing the pattern of thicker in the center and thinner at both ends. The average thickness of Glacier No. 4 is 27.6 m in 2009 and it is relative larger along the glacier flowline. The maximum value, about 105.0 m, is found near the elevation of 3 775 m a.s.l., where a closed region was formed as indicating topographic depression. To estimate glacier volume, the ice thickness map retrieved from radar data was used. The glacier boundary was determined from the GPS measurement in the same year. The interpolation algorithm was used to calculate the ice volume based on ice-thickness data. Such a method had been successfully used to calculate the ice volume of Hurd Peninsula glaciers, Livingston Island, Antarctica by Molina et al. (2007). The ice volume was calculated to be about 0.076 $km^3$ in 2009, corresponding to the water equivalent of 0.068 $km^3$, with assuming the ice density of 900 $kg{\cdot}m^{-3}$. The gridding arithmetic used to calculate the present ice volume in this paper was based on a large number of ice thickness data measured by GPR, and the result of this method was therefore reliable. In estimating the ice volume in 2009, the errors mainly came from the data coverage (representative) of the surface ice thickness data and the numbers of the measured glacier thickness data. More measured data and more representatives of the measured data will give a more precise estimated ice volume. The estimated error of the ice volume was ~±20%, which was directly related to the accuracy of the ice thickness measurement derived by error propagation.

The bedrock topographic map of Glacier No. 4 (Fig. 5) was obtained by subtracting the ice thickness from the surface topography. Contours, at 50 m spacing, of bedrock topography were constructed according to the assumptions: the ice thickness is zero at the margin of the glacier and the ice thickness in crevassed zones is lower than in nearby areas exhibiting the same surface slope but no crevasses. The bedrock of Glacier No. 4 is irregular in the tongue area, showing a clear overdeepening in the area of thickest ice, close to the ice front, but quite regular in the upper part of the glacier, which is similar to Ürümqi Glacier No. 1 (Sun et al., 2003). The bedrock topography of Glacier No. 4 is more undulating than the glacier surface, indicating that the amplitude of the bedrock undulation decreases with increasing distance above the bedrock.

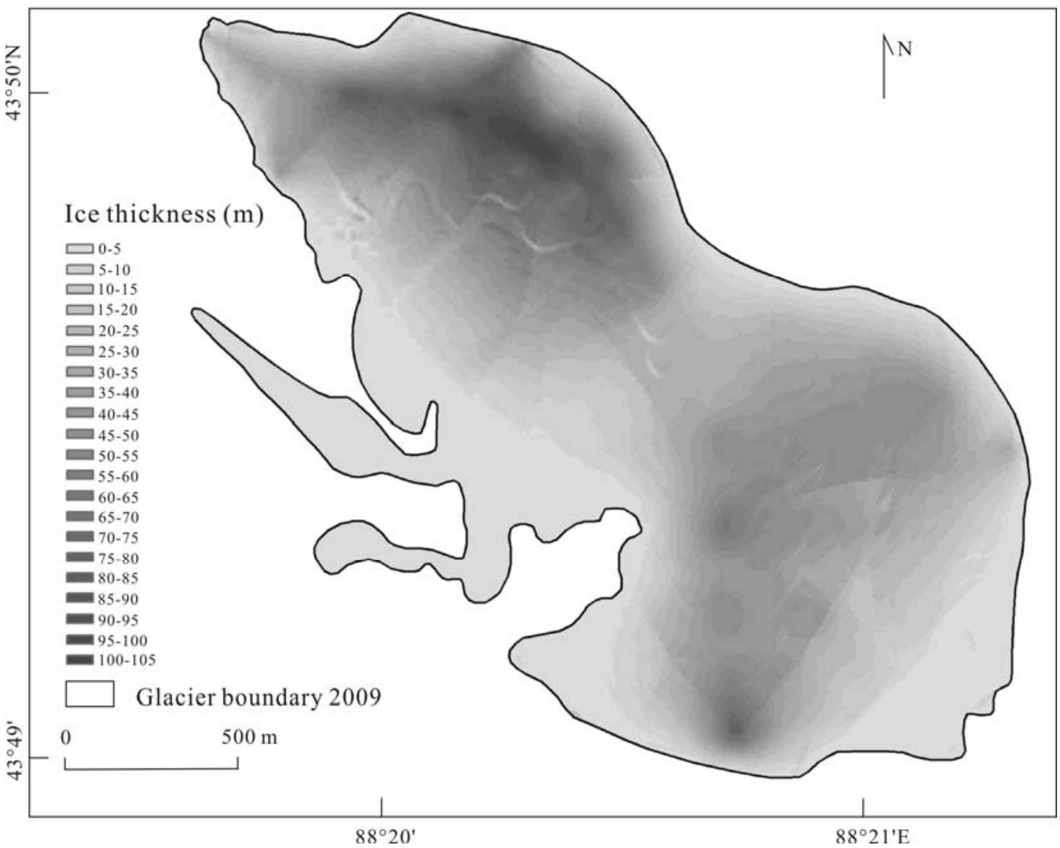


**Figure 4. Ice-thickness distribution of Glacier No. 4 of Sigong River.**

## 4 DISCUSSION AND OUTLOOK

Based on glacier volume estimated from measured values of ice thickness, several empirical algorithms have been developed to calculate ice volume from easily observed ice surface quantities (e.g., Meier and Bahr, 1996; Chen and Ohmura, 1990; Driedger and Kennard, 1986). These area-volume scaling algorithm were developed from, and possibly designed for, different volume data and were usually applied to a large sample of glaciers. Nevertheless, it might be of interest to compare the mean ice thickness calculated for one glacier with measured data. The area-volume scaling algorithm is of the form

$$V = \beta S^{\gamma} \tag{4}$$

where $V$ is the ice volume of glacier, $S$ the area, $\beta$ and $\gamma$ the coefficient, derived by using empirical, statistical or theoretical methods. The volume of Glacier No. 4 was also estimated by the empirical formula established for the glaciers in the Chinese territory (Liu et al., 2003). The empirical algorithm is based on thicknesses of six valley glaciers, five cirque glaciers, one hanging glacier, one ice cap and three cirque-hanging glaciers (area 0.46–165 $km^2$) in the Tianshan that were measured in the 1980s with a radar-sounding system designed at the Lanzhou Institute of Glaciology and Geocryology (LIGG), Chinese Academy of Sciences (LIGG, 1986). In addition, the ice thickness of seven glaciers (area 0.1–7 $km^2$) in the Qilian Mountain was estimated using topographical method (Shi, 2005). However, the difference of ice volume calculated by the empirical algorithm with the result in this study was large (-112%). Analysis indicated that the value of $\beta$ and $\gamma$ in the empirical algorithm were affected by the glacier topographic parameter (e.g., length, width; Radić et al., 2007). Especially, the parameter would differ in the different periods. The empirical algorithm used was established based on the ice thickness data measured in the 1980s; however, it has varied in the recent years due to the global warming. Therefore, a large sample of glaciers will be investigated in a future project to calculate the ice volume and an empirical formula need to be constructed for this period. The calculation of volume from the measured ice thickness data seems to be accurate way of monitoring volume change. However, the accuracy of volume changes calculated from GPR measurements is highly dependent on the accuracy of positioning and is a more cost-effective. In addition, the observation time of Glacier No. 4 is limited and we don't have drilled hole to validate the ice thickness measured by GPR. Therefore, the calculation of volume changes from surface elevation data seems to be a more cost-effective and accurate way of monitoring volume changes. This is especially true on a timescale of decades, since in the last decades GPR and GPS technology have developed rapidly and it might not be possible to revisit a site with the same measurement configuration. A field resurvey to collect ground truth for validation of calculated bedrock maps, ideally by means of drilling or else through GPR or seismic investigations, is also desirable.

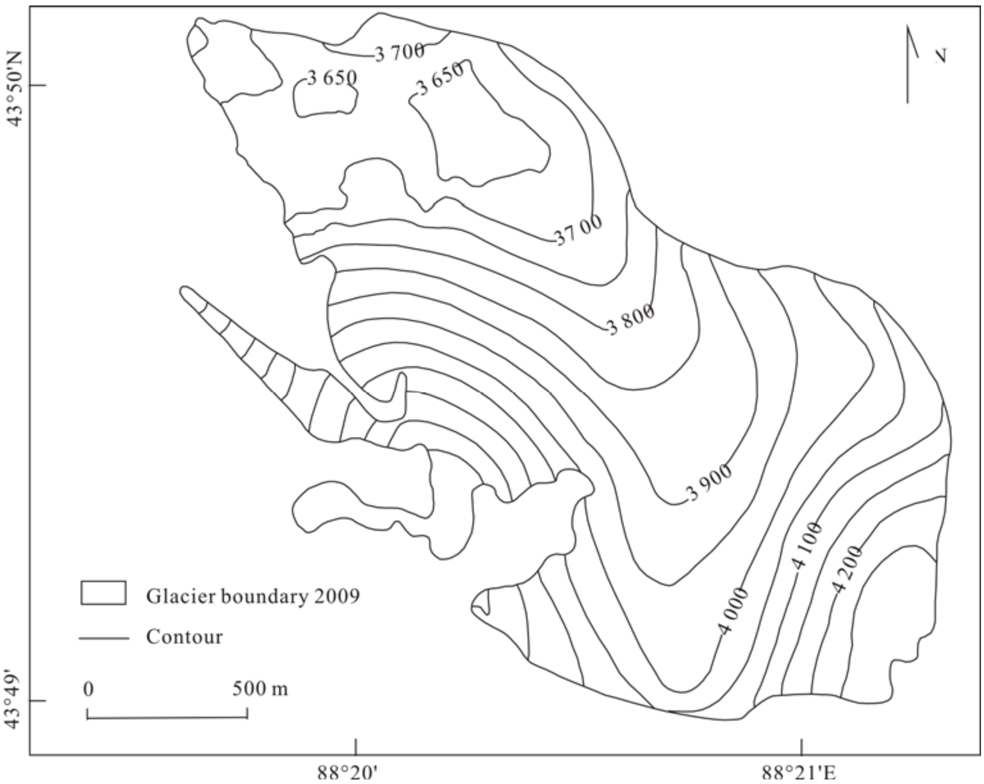


**Figure 5. Bedrock topographic map obtained by subtracting the ice thickness from the surface topographic map. Contour interval=50 m.**

Shi and Shen. (2003) have suggested that the apparent transition from warm and dry to warm and humid condition that has occurred during the last two decades is a strong indicator of climate change. Observations indicate that air temperature has increased at a rate of 0.2 ℃ per decade in the past 50 years in western China, and especially rapidly during the 1980s–1990s. The 1990s may be the warmest period not only in the past century but also in the past 1 000 years. The average air temperatures of 128 stations during the period 1987–2000 rose by 0.7 ℃ compared with the period 1961–1986 (Dong, 2002). The observed temperature at the Tianchi Meteorological Station (Fig. 6), which was located about ~10 km northwest to Glacier No. 4 and established since 1958 demonstrates an overall increase, especially during the period 2001–2007. The linear trend analysis indicated the annual mean temperature increased by approximately 0.18 ℃/10 a from 1959 to 2007.

The air temperature observed in this area is generally in phase with other parts of Tianshan. According to Aizen et al. (1997), the average increase in temperature over the central and western Tianshan was 0.1 ℃/10 a during the period 1940–1991. The value is a little lower than our observations at eastern Tianshan, which is considered a result of more rapid temperature increase after the 1980s. During the corresponding period 1959–2007, annual precipitation has been increasing gradually with the average rate of 10.54 mm/10 a. In the light of regional climatic warming and wetter, the determination of glacier volume and volume change will be an important subject of research in future. And the integration of GPR, GPS and GIS will make glaciology more dynamic, more analytical, more comprehensive, more exploratory and more predictive.

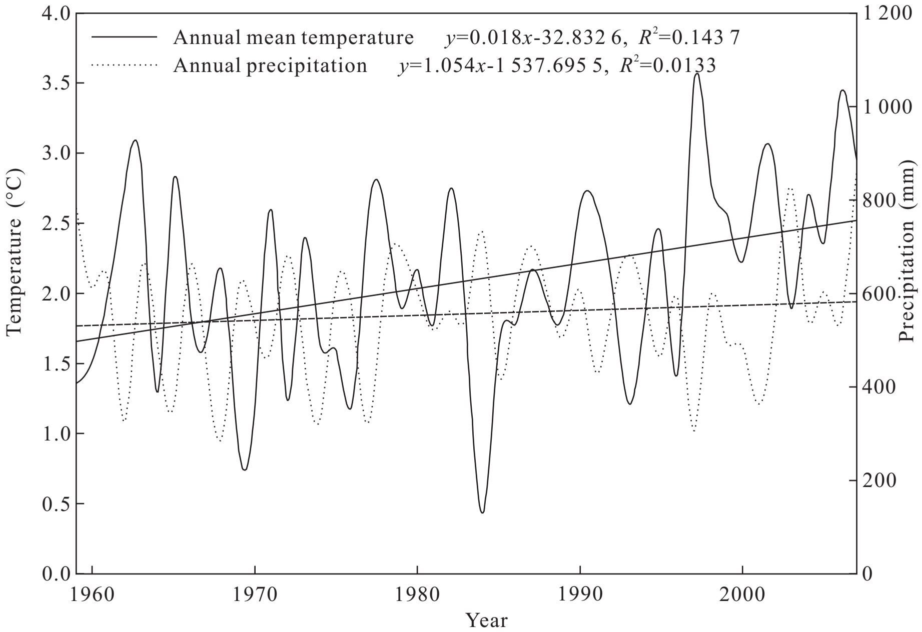


**Figure 6. Variations in annual mean temperature and annual precipitation observed at the Tianchi Meteorological Station in 1959–2007.**

**ACKNOWLEDGMENTS**

Thanks are given to Tianshan Glaciological Station for data collection. This research was jointly supported by the Funds for Creative Research Groups of China (No. 41121001), the National Natural Science Foundation of China (Nos. 41301069, 91025012 and 41101066), the SKLCS founding (Nos. SKLCS-ZZ-2012-01-01, SKLCS-ZZ-2012-01-09) and the West Light Program for Talent Cultivation of Chinese Academy of Sciences.

**REFERENCES CITED**

Aizen, V. B., Aizen, E. M., Melack, J. M., et al., 1997. Climatic and Hydrologic Changes in the Tien Shan, Central Asia. *Journal of Climate*, 10: 1393–1404

Annan, A. P., Waller, W. M., Strangway, D. W., et al., 1975. The Electromagnetic Response of a Low-Loss, Two Layer, Dielectric Earth for Horizontal Electric Dipole Excitation. *Geophysics*, 40(2): 285–298

Bahr, D. B., Meier, M. F., Peckham, S. D., 1997. The Physical Basis of Glacier Volume-Area Scaling. *Journal of Geophysical Research*, 102(B9): 20355–20362

Bauder, A., Funk, M., Gudmundsson, G. H., 2003. The Ice-Thickness Distribution of Unteraargletscher, Switzerland. *Annals of Glaciology*, 37(1): 331–336

Binder, D., Brückl, E., Roch, K. H., et al., 2009. Determination of Total Ice Volume and Ice-Thickness Distribution of Two Glaciers in the Hohen Tauern Region, Eastern Alps, from GPR Data. *Annals of Glaciology*, 50(51): 71–79

Chen, J., Ohmura, A., 1990. Estimation of Alpine Glacier Water Resources and Their Change since the 1870s. *IAHS Publ*, 193: 127–135

Dong, G. R., 2002. Environmental Characteristic of West China and Its Evolution. In: Qin, D., ed., Environmental Evolution of West China. Science Press, Beijing. 49–61 (in Chinese)

Driedger, C. L., Kennard, P. M., 1986. Glacier Volume Estimation on Cascade Volcanoes: An Analysis and Comparison with Other Methods. *Annals of Glaciology*, 8: 59–64

Funk, M., Gudmundsson, G. H., Hermann, F., 1994. Geometry of the Glacier Bed of the Unteraarglacier, Bernese Alps, Switzerland. *Zeitschrift für Gletscherkde und Glazialgeologie*, 30: 187–194

Glen, J. W., Paren, J. G., 1975. The Electrical Properties of Snow and Ice. *Journal of Glaciology*, 15: 15–37

Greuell, W., 1992. Hintereisferner, Austria: Mass-Balance Reconstruction and Numerical Modelling of the Historical Length Variations. *Journal of Glaciology*, 38: 233–244

Gudmundsson, G. H., 1999. A Three-Dimensional Numerical Model of the Confluence Area of Unteraargletscher, Bernese Alps, Switzerland. *Journal of Glaciology*, 45(150): 219–230

Haeberli, W., Wächter, H. P., Schmid, W., et al., 1982. Erste Erfahrungen Mit dem US Geological Survey—Monopuls Radioecholot im Firn, Eis und Permafrost der Schweizer

Alpen. *Z. Gletscherkd. Glazialgeol.*, 19(1): 61–72

Hubbard, A., Blatter, H., Nienow, P., et al., 1998. Comparison of a Three-Dimensional Model for Glacier Flow with Field Data from Haut Glacier d'Arolla, Switzerland. *Journal of Glaciology*, 44(147): 368–378

Hutter, K., 1983. Theoretical Glaciology. D. Reidel Publishing Company, Holland. 256–332

Jevrejeva, S., Moore, J. C., Grinsted, A., 2008. Relative Importance of Mass and Volume Changes to Global Sea Level Rise. *Journal of Geophysical Research*, 113: D08105

Kouemou, G., 2010. Rader Technology-Radar Systems for Glaciology. Vukovar, Croatia

Kovacs, A., Gow, A. J., Morey, R. M., 1995. The In-Situ Dielectric Constant of Polar Firn Revisited. *Cold Regions Science and Technology*, 23: 245–256

Lanzhou Institute of Glaciology and Geocryology (LIGG), 1986. Tien Shan Mountains (Interior Drainage Area of Junggar Basin in Northwest). In: Glacier Inventory of China. Vol. III. Science Press, Beijing (in Chinese)

Li, Z. Q., Li, K. M., Wang, L., 2010. Study on Recent Glacier Changes and Their Impact on Water Resources in Xinjiang, North Western China. *Quaternary Sciences*, 30(1): 96–106 (in Chinese with English Abstract)

Liu, S. Y., Sun, W. X., Shen, Y. P., et al., 2003. Glacier Changes since the Little Ice Age Maximum in the Western Qilian Shan, Northwest China, and Consequences of Glacier Runoff for Water Supply. *Journal of Glaciology*, 49(164): 117–124

McBratney, A. B., Webster, R., 1983. Optimal Interpolation and Isarithmic Mapping of Soil Properties: V. Co-Regionalization and Multiple Sampling Strategy. *Journal of Soil Science*, 34(1): 137–162

Meier, M. F., Bahr, D. B., 1996. Counting Glaciers: Use of Scaling Methods to Estimate the Number and Size Distribution of Glaciers of the World. *CRREL Special Repor.*, 96–27: 89–94

Molina, C., Navarro, F. J., Calvet, J., 2007. Hurd Peninsula Glaciers, Livingston, Island, Antarctica, as Indicators of Regional Warming: Ice-Volume Changes during the Period 1956–2000. *Annals of Glaciology*, 46: 43–49

Müller, F., Caflisch, T., Müller, G., 1976. Firn und Eis der Schweizer Alpen: Gletscherinventar. Zürich, Eidgenössische Technische Hochschule Zürich. Geographisches Institut Publ., Zürich. 57

Murray, T., Gooch, D. L., Stuart, G. W., 1997. Structures within the Surge Front at Bakaninbreen, Svalbard Using Ground Penetrating Radar. *Annals of Glaciology*, 24: 122–129

Narod, B. B., Clarke, G. K. C., 1994. Miniature High-Power Impulse Transmitter for Radio-Echo Sounding. *Journal of Glaciology*, 40(134): 190–194

Nye, J. F., 1965. The Flow of a Glacier in a Channel of Rectangular, Elliptic or Parabolic Cross-Section. *Journal of Glaciology*, 5(41): 661–690

Paterson, W. S. B., 1994. The Physics of Glacier (Third Edition). Pergamon Press, Oxford. 238–288

Radić, V., Hock, R., Oerlemans, J., 2007. Volume-Area Scaling vs Flowline Modeling in Glacier Volume Projections. *Annals of Glaciology*, 46: 234–240

Rivera, A., Casassa, G., Bamber, J., et al., 2005. Ice Elevation Changes of Glaciar Chico, Southern Patagonia, Using ASTER DEMs, Aerial Photographs and GPS Data. *Journal of Glaciology*, 51(172): 105–112

Robin, G. D. Q., 1975. Velocity of Radio Waves in Ice by Means of a Bore-Hole Interferometric Technique. *Journal of Glaciology*, 15(73): 151–159

Sensors and Soft Ware Inc., 1994. PulseEKKO 100 User's Guide Version 1.1. Mississauga, Ontario, Sensors and Software Inc., Technical Manual 25

Shi, Y. F., 2005. A Concise China Glacier Inventory. Shanghai Science Popularization Press, Shanghai (in Chinese)

Shi, Y. F., Shen, Y. P., et al., 2003. Discussion on the Present Climate Change from Warm-Dry to Warm-Wet in Northwest China. *Quaternary Sciences*, 23: 152–164 (in Chinese with English Abstract)

Sun, B., He, M. B., Zhang, P., et al., 2003. Determination of Ice Thickness, Subice Topography and Ice Volume at Glacier No. 1 in the Tianshan, China, by Ground Penetrating Radar. *Chinese Journal of Polar Research*, 15(1): 35–44 (in Chinese with English Abstract)

Wallinga, J., Van de Wal, R. S. W., 1998. Sensitivity of Rhonegletscher, Switzerland, to Climate Change: Experiments with a One-Dimensional Flowline Model. *Journal of Glaciology*, 44: 383–393

Wang, J. X., Wang, J., Lu, C. P., 2003. Problem of Coordinate Transformation between WGS-84 and Beijing 54. *Journal of Geodesy and Geodynamics*, 23(3): 70–73 (in Chinese)

Wang, N. L., Pu, J. C., 2009. Ice Thickness, Sounded by Ground Penetrating Radar, on the Bayi Glacier in the Qilian Mountains, China. *Journal of Glaciology and Geocryology*, 31(3): 431–435 (in Chinese with English Abstract)

Zhang, X. S., Zhu, G. C., Qian, S. L., et al., 1985. Radar Measuring Ice Thickness of Glacier No. 1 at the Source of Urumqi River, Tianshan. *Journal of Glaciology and Geocryology*, 7(2): 153–162 (in Chinese with English Abstract)